World Conference on Timber Engineering Oslo 2023

COMPARISON BETWEEN EXPERIMENTAL RESULTS AND DESIGN EQUATIONS OF ARTIFICIALLY DEGRADED SINGLE STEP JOINTS

Daniel F. Lima[1], Jorge M. Branco[2], Lina Nunes[3]

ABSTRACT: In the case of interventions in existing buildings, the assessment of timber elements and joints, such as the Single Step Joint, is a challenge for engineers, especially when timber presents signs of biological degradation. In this context, many roof structures are subject to unnecessary substitutions due to the lack of knowledge about the behaviour of these types of joints, and specially the consequences of eventual biological attacks. This study aims to evaluate the residual shear strength of Single Step Joints artificially degraded by wood boring insects from the Anobiidae family (e.g. *Anobium punctatum)*. To achieve the established objectives, destructive tests were carried out on undamaged (reference level) and artificially degraded Single Step Joint specimens, varying the level of degradation. The results were analysed in terms of degradation level and compared with the results obtained with design equations for this type of joint found in the literature. From the analysis of the results, it was possible to observe the tendency of reduction of the shear strength with the increase of the degradation level.

KEYWORDS: Single Step Joint, Traditional carpentry connections, Biological degradation, *Anobium punctatum*

1 INTRODUCTION

Applying wood as a building material requires special attention, especially when it is used for structural functions. Despite its high complexity, when applied correctly with adequate protection and maintenance, wood is one of the most efficient building materials.

Like other natural organic materials, wood is subject to biological degradation, where the main agents are fungi and insects. Despite its recognized tradition and presence in the built heritage, knowledge about the biological degradation process of wooden structures, as well as its impacts on the service life of buildings, remains, to a certain extent, unknown.

Concerning degradation caused by insects, in countries with temperate climates, subterranean termites and woodboring beetles stand out, due to their ability to cause severe damage to structural elements with a consequent reduction in the service life of the structure [1]. On the other hand, anobiids (like the common furniture beetle or woodworm) represent a considerable challenge since the quantification of their impact on the mechanical strength of structural elements still raises many questions.

Typically, woodboring insects' infestation is assessed by the visual inspection of the element. In this case, the intensity of infestation is quantified by the density of apparent exit holes on the element surface. However, the diffuse attack of this insect makes the assessment of damage intensity more difficult [2]. In fact, despite being the most recurrent, this evaluation method presents too many uncertainties, since the number of internal galleries drilled by the insects is greater than the surface exit holes, which can lead to an underestimation of the level of degradation [3,4].

Regarding the reduction of the mechanical capacity caused by the anobiid infestation, in general, it is considered in the structural verification of old structural elements either by the reduction of the cross-section of the element (considering that the degraded zone does not present any strength) or assuming reduced mechanical properties for that element [5,6]. However, there is a clear lack of studies that can serve as a basis for engineers to adopt the appropriate reduction factors.

The lack of knowledge, combined with the difficulty in assessing the extent and severity of damage, is responsible for many unnecessary replacements of structures that could be subjected to curative treatments and/or reinforcements. In this context, timber roofs represent a great challenge, being common to find elements and joints degraded by insects and fungi due to their constant contact with the supporting masonry [7].

The present paper aims to discuss the impact of anobiids on the shear strength of Single Step Joints. Previously, Single Step Joint design equations were studied by [8] and will be used as reference to identify the need of introducing a safety factor for woodworm degraded elements.

2 Traditional Carpentry Joints

Carpentry connections are usually composed of notched joints and are traditionally used to connect the rafter and

[1] Daniel F. Lima, ISISE, University of Minho, Portugal, daniel.asmf.lima@gmail.com
[2] Jorge M. Branco, ISISE, University of Minho, Portugal, jbranco@civil.uminho.pt
[3] Lina Nunes, National Laboratory for Civil Engineering (LNEC), Portugal, linanunes@lnec.pt

the tie beam in timber trusses, where the stresses are transferred between the elements by axial compression and/or friction [9,10]. Over time, geometric variants of this type of connection have been developed, standing out the Single Step Joint and the Double Step Joint, being the former the most common due to their simplicity and easier manufacturing process.

Among Single Step Joints, exist three main families: the Geometrical Configuration Ideal Design (GCID), the Geometrical Configuration Perpendicular to the Rafter (GCPR), and the Geometrical Configuration Perpendicular to the Tie Beam (GCPTB) [11]. The difference between the three families relies on the inclination of the front notch (α) in relation to the rafter skew angle (β), where the GCID has α equivalent to β/2, the GCPR has α equivalent to β and the GCPTB has α=0º (figure 2.1).

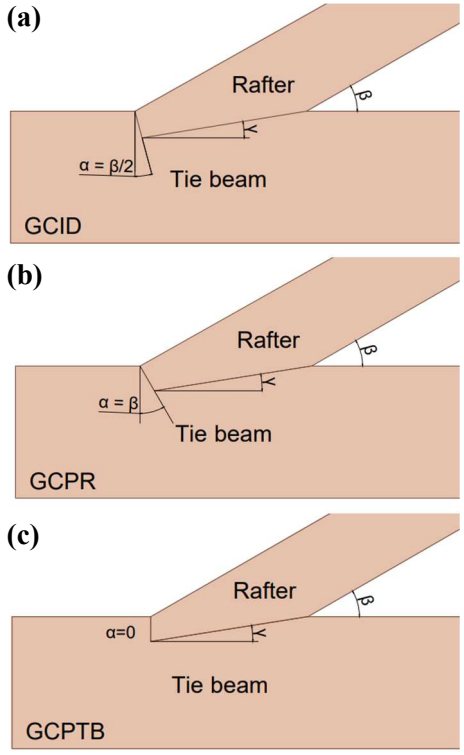

Figure 2.1: *Main SSJ geometrical variations. (a) Geometrical Configuration Ideal Design (GCID); (b) Geometrical Configuration Perpendicular to the Rafter (GCPR); (c) Geometrical Configuration Perpendicular to the Tie Beam (GCPTB)*

With the development of new precise technologies (for example CNC) and because it is considered the most efficient, the GCID is the recommended. However, due to the lack of accurate carpenter tools in the past, the other two configurations are commonly found in older constructions with low quality (in terms of carpenters' skills) [8].

Two possible failure modes are considered for the SSJ: shear parallel to the fibres at heel depth and crushing parallel to the fibres at the front notch [7]. However, Verbist et al. [8] questioned the consideration of crushing at the front notch as a failure mode for the SSJ, since the crushing will only cause the densification of the wood fibres and consequent deformations at the joint, being shear the final failure mode.

In recent decades, several studies have addressed the mechanical behaviour of Single Step Joint, for example, Verbist et al. [8], Branco et al. [7], Munafò et al. [12], Palma et al. [13], among others. Despite being traditional and commonly found in constructions, both in new and older constructions, the SSJ continue to present knowledge gaps to be explored.

3 Materials and methods

3.1 SSJ specimens

The Single Step Joints specimens with structural dimensions used on this study were made of scots pine (*Pinus sylvestris* L.), acquired in Northern Spain, followed the Geometrical Configuration Perpendicular to the Tie Beam (GCPTB), consequently, the front notch perpendicular to the tie beam grain (α=0°). Additionally, a skew angle between the tie beam and the rafter of 30° ($\beta = 30°$), a heel depth of 30mm ($h_V = 30mm$), a width of 100mm ($b = 100mm$), and a heel length of 100mm ($l_V = 100mm$) were adopted (figure 3.1). The geometry of the specimens was defined based on the results obtained by [8], with the aim to induce failure by shear at the heel depth.

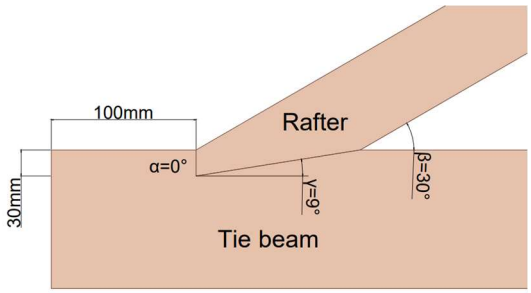

Figure 3.1: *Geometry adopted for the SSJ specimen*

Before carrying out the procedures of the experimental campaign, the specimens were stored in a climatic chamber at a constant temperature of 20 ± 1°C and a relative humidity of 60 ± 5% until mass stabilization (i.e., difference ≤ 0.1% between consecutive measurements, EN 13183 [14]]). Under these climatic conditions, the equilibrium moisture content of the wood should be approximately 12% [15]. Additionally, density ($\rho_{12\%}$) was determined following the procedures of NP 616 [16].

3.2 Visual grading

To ensure a control quality of the wood and to confirm the strength class in accordance with EN 338 [17], a visual grading of the specimens was carried out, based on a photographic survey followed by the application of the procedure described by UNE 56544 [18]. Therefore, all the defects and singularities referred to in the applied standard were duly identified and measured, namely: knots, resin pockets, fissures, wane, biological damage,

distortions, and width of the annual rings, among others. For visual inspections on structural elements with a rectangular cross-section width greater than 70mm, UNE 56544 [18] defines only one quality class named MEG (*Madera Estructural de Gruesa escuadría*). The quality class is correlated with the strength class (EN 338 [17]) using EN 1912 [19], which establishes that the scots pine classified as MEG quality, with origin in Spain, fits within strength class C22.

3.3 Shear test parallel to grain performed on small specimens

Additionally, the shear strength parallel to grain of the wood used in the SSJ tests was obtained out based on shear tests on small specimens. The test method was adopted according to the recommendations of the American standard ASTM D143 [20]. The test was performed on 50 by 50 by 63mm defect-free specimens to obtain failure in the 50 by 50mm section, as shown in figure 3.2.
The test was carried out with a load application controlled by the displacement of the actuator at a constant rate of 0.6 mm/min until failure.

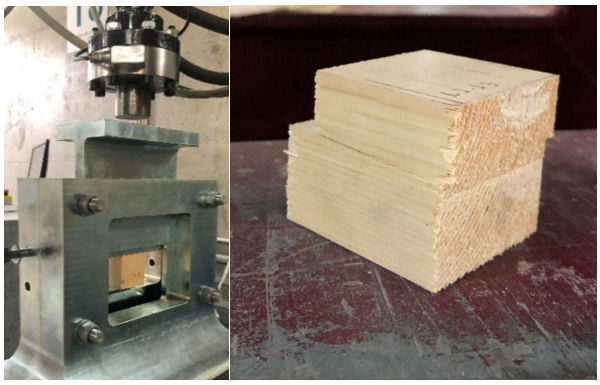

Figure 3.2: *Shear tests parallel to the grain performed on small specimens*

The shear strength was calculated using the Equation (1).

$$f_{v,SP} = \frac{N}{A_v} \quad (1)$$

Where $f_{v,SP}$ is the shear strength (MPa), N is the maximum load recorded by the load cell (N), and A_v is the shear-resistant area (mm^2) measured for each specimen after the test.
In total, 88 specimens were tested, and the value of the 5th percentile was adopted as the characteristic shear strength. All specimens used in those tests were stored in a climatic chamber at a constant temperature of 20 ± 1°C and a relative humidity of 60 ± 5% until mass stabilization and density ($\rho_{12\%}$) was determined following the procedures of NP 616 [16].

3.4 Simulation of the degradation

The degradation by anobiids was simulated by manual drilling in the direction parallel to the grain on the tie beam-end element [21]. The dimensions of the perforated galleries were approximately 2 mm in diameter and 100 mm in length, since the furniture beetle normally makes circular galleries of 1 to 3 mm in diameter [15], and the length of the tie beam-end is 100 mm.
Three different levels of degradation were adopted (DL-I, DL-II, and DL-III) varying the density of perforated galleries (1.67 holes/cm^2, 3.33 holes/cm^2, and 4.00 holes/cm^2), seeking to achieve realistic degradation levels.

3.5 SSJ Tie beam-end shear test

The destructive test consists of applying an increasing normal load (N_{rafter}) on the rafter, controlled by the actuator displacement with a constant rate of 0.01 mm/s (figure 3.3). The normal load (N_{rafter}) results in compressive stresses on the surfaces of the SSJ (compression parallel to the grain on the Front Notch and perpendicular to the grain on the Bottom Notch) and shear stresses on the tie beam-end.
The expected failure mode of the specimen is the shear failure at the tie beam-end, induced by the low skew angle (β=30°) and reduced ratio between the heel depth and the shear length (lv/tv≤6) (section 3.1) [8].

Figure 3.3: *SSJ Tie beam-end shear test*

Forty specimens were tested: 4 undamaged specimens (i.e., reference) and 12 specimens for each of the three levels of degradation (section 3.4).

3.6 Design rafter load-bearing capacity ($N_{rafter,Rd}$)

In this study, Equation (2) [8] will be used to verify the design rafter load-bearing capacity ($N_{rafter,Rd}$).

$$N_{rafter,Rd} \leq k_{v,red} \cdot f_{v,k} \frac{k_{mod}}{\gamma_M} \cdot \frac{b.k_{cr}.\mathrm{l_{v,eff}}}{cos\beta} \quad (2)$$

Where, $k_{v,red}$ is the reduction factor considering the non-uniform shear stress distribution, $f_{v,k}$ is the characteristic shear resistance, k_{mod} is the modification factor considering duration of load and moisture content, γ_M is the partial factor for wood properties, b is the width, k_{cr} is reducer factor considering the eeccentricity between the joint and the support of the tie beam, $\mathrm{l_{v,eff}}$ is the effective shear length, and β is the skew angle between the rafter and tie beam.

4 RESULTS AND DISCUSSION

4.1 Visual grading

From the visual grading, it was possible to identify a series of natural defects inherent to the sawn wood. The most frequent defects were knots and drying fissures. However, all specimens submitted to the tests comply with the verifications established in UNE 56544 [18] and fall within the MEG quality class. Thus, applying the correlation from EN 1912 [19], the timber tested in this study was classified as C22. Moreover, EN 338 [17] establishes that the characteristic shear resistance of softwood classified as C22 is 3.8 MPa.

4.2 Shear test parallel to grain performed on small specimens

The results of the shear tests on small specimens and quantification of density, are presented in table 4.1.
The shear strength values varied between 5.42 MPa and 8.01 MPa, with an average of 6.59 MPa and a coefficient of variation of 8.88%. The characteristic shear strength parallel to the grain obtained on these tests is 5.66 MPa (5th percentile).
Regarding the density of the specimens, the values vary between 405.0 kg/m^3 and 566.3 kg/m^3, with an average of 501.6 kg/m^3. The EN 384 [22] standard considers the value of the 5th percentile of the sample as the characteristic density of wood (ρ_k). In the case of the present study, 419.9 kg/m³.

***Table 4.1**: Shear tests parallel to the grain and density results for the 88 tested specimens*

	Shear strength ($f_{v,SP}$)	**Density ($\rho_{12\%}$)**
Max. Value	8.01 MPa	566.3 kg/m^3
Min. Value	5.42 MPa	405.0 kg/m^3
Average	6.59 MPa	501.6 kg/m^3
Stand. dev.	0.58 MPa	38.6 kg/m^3
C.V.	8.88%	7.69%
5th percentile	5.66 MPa	419.9 kg/m^3

4.3 Design rafter load-bearing capacity ($N_{rafter,Rd}$)

In this study, two different theoretical SSJ shear strength will be considered. The first, is considering the characteristic shear resistance as the value obtained through the visual grading, while the second considers the shear test on small specimens' 5th percentile value. Thus, the two characteristics shear strength adopted to apply on Equation (2) are 3.8 MPa and 5.42 MPa, respectively.
Regarding the other inputs for Equation (2), table 4.2 presents the values adopted and the references used to adopt it.

***Table 4.2:** Input values and references adopted for Equation (2)*

	Value	**References**
$k_{v,red}$	0.96	[8,23]
k_{mod}	0.9	[24]
γ_M	1.3	[24]
k_{cr}	1	[8]
$\mathrm{l_{v,eff}}$	$\min(l_v; 8h_v) = 100mm$	Section 3.1,
b	100mm	Section 3.1
β	30°	Section 3.1

Therefore, the two values for the design rafter load-bearing capacity ($N_{rafter,Rd}$) obtained are 27.7 kN (for $f_{v,k}$=3.8 MPa) and 39.5 kN (for $f_{v,k}$=5.42 MPa).

4.4 SSJ Tie beam-end shear test

Table 4.3 presents the results obtained in the SSJ tie beam-end shear tests and the quantification of density.

***Table 4.3:** Summary of the results obtained from the quantification of the density and the SSJ tie beam-end shear tests*

Group		REF	DL-I	DL-II	DL-III
N°		4	12	12	12
$\boldsymbol{\rho_{12}}$ [kg/m³]	$\bar{X}$	529	514	511	493
	σ	26	50	41	52
	C.V.	4.9%	9.8%	7.9%	10.6%
$\boldsymbol{N_{rafter,SSJ}}$ [kN]	$\bar{X}$	43.4	45.3	39.6	38.6
	σ	2.3	8.2	3.4	5.2
	C.V.	5.2%	18.2%	8.7%	13.5%

$\bar{\boldsymbol{X}}$ – Average; $\boldsymbol{\sigma}$ – Standard Deviation; C.V. – Coefficient of variation; $\boldsymbol{\rho_{12}}$ – Density corrected to a 12% moisture content; $\boldsymbol{N_{rafter,SSJ}}$ – Experimental rafter load-bearing capacity

As expected, all 40 specimens presented shear failure without crushing parallel to the grain at the front notch or perpendicular to the grain at the bottom notch (figure 4.1).

Figure 4.1: *Characteristic shear failure on the tie beam-end observed in the 40 SSJ specimens tested.*

Regarding the rafter load-bearing capacity, firstly, it was verified that the distribution of the results fit the normal distribution through the Shapiro-Wilk test (p-value = 0.14).

As previously mentioned, drilling densities equivalent to 1.66 holes/cm², 3.33 holes/cm², and 4.00 holes/cm² were adopted, corresponding to groups DL-I, DL-II, and DL-III, respectively. Figure 4.2 shows the bar chart that graphically represents the shear strength mean values and the respective standard deviations of the degradation groups.

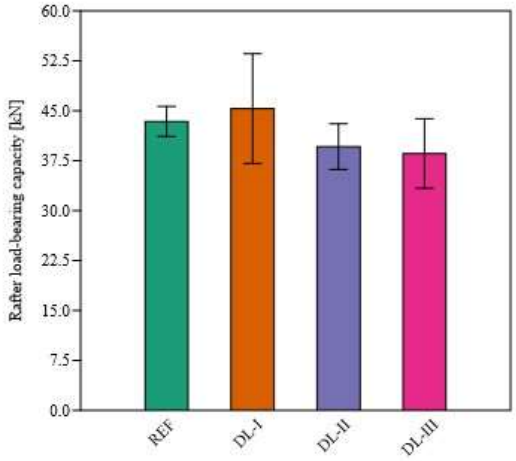

Figure 4.2: *Bar chart of the results of the tie beam-end shear tests*

Through the analysis of table 4.3 and figure 4.2, it is possible to observe that the group with the lowest level of degradation (DL-I) presented superior results (+4%, on average) compared to the reference group (REF). Therefore, it is possible to conclude that, at this level, the degradation was not enough to cause significant damage to the specimen and, in this group, other properties such as density and wood natural variability, were more determinant in the shear strength parallel to the grain. On the other hand, the higher two levels of degradation showed lower tests results than the reference group (-10% and -11%, on average), demonstrating the influence of the drilled galleries.

4.5 Comparison between experimental results and design equations

Table 4.3 presents the comparison between the theoretical rafter load-bearing capacity, calculated from Equation (2), and the average results of the SSJ tie beam-end shear tests. The comparison is made in terms of the relative variation $\Delta_{rel,rafter}$ (%). In table 4.4, $N_{rafter,Rd1}$ represents the design rafter load-bearing capacity considering the results of the visual grading, while $N_{rafter,Rd2}$ considers the results of the shear test on small specimens.

Table 4.4: *Experimental results divided by drilling density, design equation results, and relative variation between the experimental and theoretical results.*

	N_{rafter} [kN]	$\Delta_{rel,rafter1}$	$\Delta_{rel,rafter2}$
$N_{rafter,Rd1}$	27.7	-	-
$N_{rafter,Rd2}$	39.5	-	-
$N_{rafter,SSJ,REF}$	43.4	56.6%	9.8%
$N_{rafter,SSJ,DL-I}$	45.3	63.6%	14.7%
$N_{rafter,SSJ,DL-II}$	39.6	43.0%	0.2%
$N_{rafter,SSJ,DL-III}$	38.6	39.2%	-2.4%

From table 4.4, it is possible to observe the reliability of the design equation when considering the shear test on small specimens performed on this study ($\Delta_{rel,rafter2}$ between 14.7% and -2.4%), while the C22 grading shows theoretical results much lower than the experimental results ($\Delta_{rel,rafter}$ between 63.6% and 39.2%).
The results are exposed in figure 4.3 in a scatter plot, where the blue line represents the $N_{rafter,Rd1}$ and the red line $N_{rafter,Rd2}$.

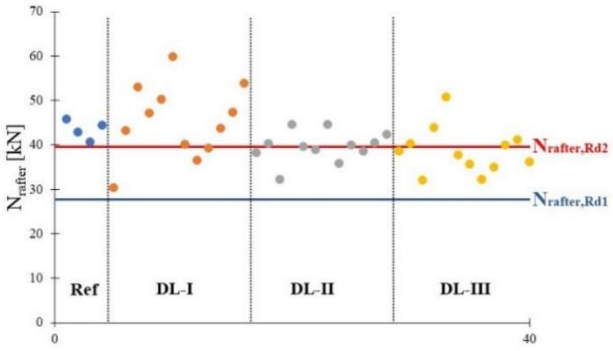

Figure 4.3: *Tests results separated by level of degradation and comparison with design values.*

Analysing the graph exposed in figure 4.3, it is possible to infer that, when considering the strength class C22 proposed by EN 1912 ($N_{rafter,Rd1}$), all 40 specimens presented higher values, discarding the need to consider a reduction factor due to degradation by anobiids. On the other hand, when considering the value of the characteristic resistance obtained by shear test on small specimens ($N_{rafter,Rd2}$), it is possible to notice that all the reference specimens (without degradation) presented

values slightly higher than those obtained by applying the equation (2) and that the number of tests with values below the $N_{rafter,Rd2}$ line increase with increasing of the level of degradation (3 tests for the DL-I, 5 for the DL-II and 7 for the DL-III level).

Therefore, based on the analysis of table 4.4 and figure 4.5, it can be concluded that although the shear test on small specimens more accurately represents the value of the wood's characteristic shear strength ($f_{v,k}$), it indicates the need to assign a reduction factor due to biological degradation to Equation (2) for the correct determination of the design rafter load-bearing capacity of SSJ degraded by anobiids.

5 CONCLUSIONS

From the results of the experimental campaign and the application of the design equation, it is possible to infer that, when considering the strength grading C22 for scots pine, the degradation achieved in this study is not enough to reduce the load-carrying capacity to the point that element replacement is required, confirming the theory that many replacements are unnecessary [3]. On the other hand, shear test on small specimens presented a more precise characteristic shear strength, and, in this case, it is clear the tendency of reducing the shear strength with the increase of the level of degradation and the necessity to impose a reduction factor to the design equation due to biological degradation. Thus, for future developments, it is intended to establish a correlation between the level of degradation by anobiids and the residual shear strength of SSJ, with the aim to propose values for that reduction factor.

ACKNOWLEDGEMENT

This work is supported by national funds through FCT – Fundação para a Ciência e a Tecnologia within a Ph.D. scholarship within MIT Portugal Program (PRT/BD/152833/2021).

REFERENCES

[1] Eaton RA, Hale MDC. Wood: decay, pests, and protection. 1st ed. London: Chapman & Hall; 1993.

[2] Reinprecht L. Wood deterioration, protection and maintenance. Chichester: John Wiley & Sons Ltd; 2016.

[3] Parracha JL, Pereira MFC, Maurício A, Machado JS, Faria P, Nunes L. A semi-destructive assessment method to estimate the residual strength of maritime pine structural elements degraded by anobiids. Materials and Structures/Materiaux et Constructions 2019;52. https://doi.org/10.1617/s11527-019-1354-9.

[4] Parracha J, Pereira M, Maurício A, Faria P, Lima DF, Tenório M, et al. Assessment of the density loss in anobiid infested pine using x-ray micro-computed tomography. Buildings 2021;11. https://doi.org/10.3390/buildings11040173.

[5] Cruz H, Yeomans D, Tsakanika E, Macchioni N, Jorissen A, Touza M, et al. Guidelines for on-site assessment of historic timber structures. International Journal of Architectural Heritage 2015;9:277–89. https://doi.org/10.1080/15583058.2013.774070.

[6] UNI 11119. Cultural heritage – Wooden artefacts – Load bearing structures of buildings – On site inspection for the diagnosis of timber members. Milan, UNI; 2004.

[7] Branco JM, Verbist M, Descamps T. Design of three Step Joint typologies: Review of European standardized approaches. Eng Struct 2018;174:573–85. https://doi.org/10.1016/j.engstruct.2018.06.073.

[8] Verbist M, Branco JM, Poletti E, Descamps T, Lourenço PB. Single Step Joint: overview of European standardized approaches and experimentations. Materials and Structures/Materiaux et Constructions 2017;50. https://doi.org/10.1617/s11527-017-1028-4.

[9] Branco JM. Influence of the joints stiffness in the monotonic and cyclic behaviour of traditional timber trusses. Assessment of the efficacy of different strengthening techniques. Doctoral Thesis. University of Minho, 2008.

[10] Yeomans D. The repair of historic timber structures. Thomas Telford Ltd; 2003.

[11] Oslet G. Encyclopédie théorique & pratique des connaissances civiles & militaires - Traité de charpente en bois. Paris: 1890.

[12] Munafò P, Stazi F, Tassi C, Davì F. Experimentation on historic timber trusses to identify repair techniques compliant with the original structural–constructive conception. Constr Build Mater 2015; 87:54–66. https://doi.org/10.1016/j.conbuildmat.2015.03.086.

[13] Palma P, Ferreira J, Cruz H. Monotonic tests of structural carpentry joints. WCTE2010 - World conference on timber engineering, Trento: 2010.

[14] EN 13183. Moisture content of a piece of sawn timber. Brussels, Belgium: European Committee for Standardization CEN; 2012.

[15] Cruz H, Jones D, Nunes L. Wood. Materials for Construction and Civil Engineering, Cham: Springer International Publishing; 2015, p. 557–83. https://doi.org/10.1007/978-3-319-08236-3_12.

[16] NP 616. Madeiras. Definição da massa volúmica. IGPAI, Lisbon; 1973.

[17] EN 338. Structural timber - Strength classes. Brussels, Belgium: European Committee for Standardization CEN; 2016.

[18] UNE 56544. Clasificación visual de la madera aserrada para uso estructural - Madera de coníferas. AENOR, Madrid; 2011.

[19] EN 1912. Structural timber. Strength classes. Assignment of visual grades and species. Brussels, Belgium: European Committee for Standardization CEN; 2012.

[20] ASTM D143. Standard Methods of Testing Small Clear Specimens of Timber. ASTM Annual Book of Standards, West Conshohocken; 2021.

[21] Lima DF. Estruturas antigas de casquinha. Avaliação do impacto do caruncho pequeno por

simulação da degradação. Master thesis. University of Minho, 2022.
[22] EN 384. Structural timber - Determination of characteristic values of mechanical properties and density. Brussels, Belgium: European Committee for Standardization CEN; 2016.
[23] Verbist M, Branco JM, Descamps T. Cohesive zone models of single step joint damaged due to the shear crack. 6th European Conference on Computational Mechanics (ECCM 6), Glasgow: 2018, p. 1257–68.
[24] EN 1995-1-1. Eurocode 5 – Design of timber structures – Part 1.1: General – Common rules and rules for buildings. Brussels, Belgium: European Committee for Standardization CEN; 2004.